

Article

P21 Overexpression Promotes Cell Death and Induces Senescence in Human Glioblastoma

Moustafa A. Mansour ^{1,2*}, Masum Rahman ¹, Ahmed A. Ayad ³, Arthur Warrington¹ and Terry C. Burns ^{1*}

¹ Department of Neurologic Surgery, Mayo Clinic, Rochester MN, USA

² Center of Neurogenetics and Cancer Biology, Harvard Medical School, Cambridge MA, USA

³ Department of Neurologic Surgery, Al-Azhar Faculty of Medicine, Cairo, Egypt

* Correspondence: Burns.terry@mayo.edu (TCB); Moustafa.medavatar@gmail.com or MAMansour@mgh.harvard.edu (MAM).

Simple Summary: Current standard care for high-grade glioma involves maximal safe resection followed by chemoradiation. Recent studies showed that surviving cancer cells with an initially senescent phenotype following chemoradiation could escape senescence over time, giving rise to tumor cells that were more aggressive and resilient. Therefore, more powerful approaches are needed to either keep these glioma-initiating cells in a senescent state for longer or to eliminate these senescent cells prior to tumor recurrence. In this study, we demonstrate that P21 overexpression induces high levels of apoptosis in multiple human glioma cell lines and, in surviving cells, promotes cell cycle arrest and senescent gene expression. Additionally, we demonstrate that P21 overexpression induces senescence more rapidly and stably than irradiation of human glioblastoma cells. Finally, we find that P21-overexpressing glioma cells selectively depend upon Bcl-xL to avoid apoptotic cell death.

Abstract: High-grade gliomas are the most common and aggressive adult primary brain tumors with a median survival of only 12-15 months. Current standard therapy consists of maximal safe surgical resection followed by DNA-damaging agents, such as irradiation and chemotherapy that can delay but not prevent inevitable recurrence. Some have interpreted glioma recurrence as evidence of glioma stem cells which persist in a relatively quiescent state after irradiation and chemotherapy, before the ultimate cell cycle re-entry and glioma recurrence. Conversely, latent cancer cells with a therapy-induced senescent phenotype have been shown to escape senescence, giving rise to more aggressive stem-like tumor cells than those present in the original tumor. Therefore, approaches are needed to either eliminate or keep these glioma initiating cells in a senescent state for longer time to prolong survival. In our current study, we demonstrate that the radiation-induced cell cycle inhibitor P21 can provide a powerful route to induce cell death in short term explants of PDXs derived from three molecularly diverse human gliomas. Additionally, cells not killed by P21 overexpression were maintained in a stable senescent state for longer than control cells. Collectively, these data suggest that P21 activation may provide an attractive therapeutic target to improve therapeutic outcomes.

Keywords: P21; CDKN1A; glioblastoma; senescence; cancer senescence; gene overexpression; gene knock-in; CRISPR/Cas9; dCas; dCas-VPR

1. Introduction

Senescence is the process by which cells stop dividing and enter a state of growth arrest without undergoing cell death. Cellular senescence is a key component of human aging that can be induced by unrepaired DNA damage or other cellular stresses [1,2]. Senescence is a key mechanism of tumor suppression that may be mediated by the DNA damage response or via key oncogenes, such as ras, cyclin E, raf, and E2F3 [3,4,5]. The tumor-suppressive impact of senescence may result from directly inhibiting tumor proliferation or by stimulating an immune response against malignant cells. The role of

senescence in tumor suppression is supported in part by a higher percentage of senescent cells in pre-malignant lesions than malignant lesions, suggesting a role of senescence in blocking cancer progression [6,7,8]. Glioblastoma (GBM) is a fatal infiltrative brain tumor for which standard treatment includes maximal surgical resection followed by irradiation and alkylating chemotherapy, typically with Temozolomide (TMZ) [9]. Unfortunately, recurrence is inevitable, suggesting failure of irradiation and TMZ to maintain senescence in glioblastoma cells. Therefore, avenues to either eliminate senescent cells after therapy or prevent senescent escape could improve outcomes.

Activation of the p53/P21^{WAF1/CIP1} and p16^{INK4A}/pRB tumor suppressor pathways play a central role in regulating senescence in normal mammalian cells, but cancer cells dysregulate these genes to maintain their malignant features of continuous proliferation and invasion [10]. For example; homozygous deletion of CDKN2A, which encodes p16, is pathognomonic for increased aggressiveness in glioma and other cancers [11,12]. P21 is a potent cyclin-dependent kinase inhibitor (CKI) that binds to and inhibits the activity of cyclin-CDK2, -CDK1, and -CDK4/6 complexes, and thus functions as a regulator of cell cycle progression at G1 and S phase [13,14]. Although cell cycle arrest is a cardinal feature of senescence, whether externally inducing cell cycle arrest can induce other features of senescence is unclear. Although P21 is a well-characterized marker of senescence, the mechanistic role of P21 in glioblastoma survival and therapy-induced senescence has not been rigorously evaluated. P21 has been reported to have paradoxically cancer-promoting impacts in certain contexts. Here, we demonstrate that P21 overexpression induces high levels of apoptosis in multiple human glioma cells lines, and in surviving cells, promotes cell cycle arrest and senescent gene expression. Conversely, P21 downregulation promotes survival and proliferation. Additionally, we demonstrate that P21 overexpression induces senescence more rapidly and stably than irradiation of human glioblastoma cells. As previously demonstrated with radiation-induced senescence, we find that P21-overexpressing glioma cells are selectively dependent upon Bcl-XL to avoid apoptotic cell death.

2. Results

2.1. Radiation induces senescent-like gene expression in a dose-dependent manner.

Radiation is well known to induce senescence and P21 upregulation. To determine if the level of P21 expression correlates with radiation-induced senescent induction in a dose-dependent manner, we used three human glioblastoma cell lines with divergent molecular features (**Table 1**). Each cell line was treated with varying doses of radiation from 0-15Gy. mRNA was isolated and used to evaluate gene expression of P21, GLB-1 (Senescence-specific beta-galactosidase), and ki-67 (Proliferation marker; **Figure 1 and Supplementary Figure 1**). We found that both P21 and GLB-1 expression positively correlate with radiation dose (**Figure 1A, B and Supplementary Figure 1A, B**) while ki-67 inversely correlates with radiation dose (**Figure 1A, C and Supplementary Figure 1A, C**) suggesting a positive correlation between P21 and senescence, and a negative correlation between P21 and proliferation.

Table 1. Genetic and molecular characteristics of the 3 different GBM cell lines (GBM6, GBM39, and GBM164) used for experiments shown in our current study.

Cell Line	6	39	164
Sex	<i>Male</i>	<i>Male</i>	<i>Female</i>
Age	<i>65</i>	<i>51</i>	<i>38</i>
Recurrence Status	<i>Primary</i>	<i>Primary</i>	<i>Primary</i>
MGMT Methylation	<i>U</i>	<i>M</i>	<i>M</i>
Sub-type	<i>Classical</i>	<i>Mesenchymal</i>	<i>Proneural</i>
IDH-1	-	-	<i>Mh</i>
CDKN2A	<i>LL</i>	<i>L</i>	<i>LL</i>
PTEN	<i>L</i>	<i>LM</i>	<i>L</i>
EGFR	<i>A (V3)</i>	<i>A (V3)</i>	-
TP53	<i>M</i>	-	-
Met.	<i>A</i>	<i>A</i>	<i>A</i>
TERT Prom.	<i>M</i>	<i>M</i>	-
Others	-	<i>MDM4 & PIKC32B Amp</i>	<i>PDGFR Amp; NF1 loss; ATRX trunc.</i>

*M=Mutant

*A=Amplified or net gain (>2n)

*L=Loss

*LL= Homozygous deletion

*Subtypes: Classical (Clas), Mesenchymal (Mes), Proneural (P), Not determined (ND)

*h heterozygous IDH R132H mutation

*v2, v3 = EGFR variants.

Data were generated and collected from the c-bio portal as in [38].

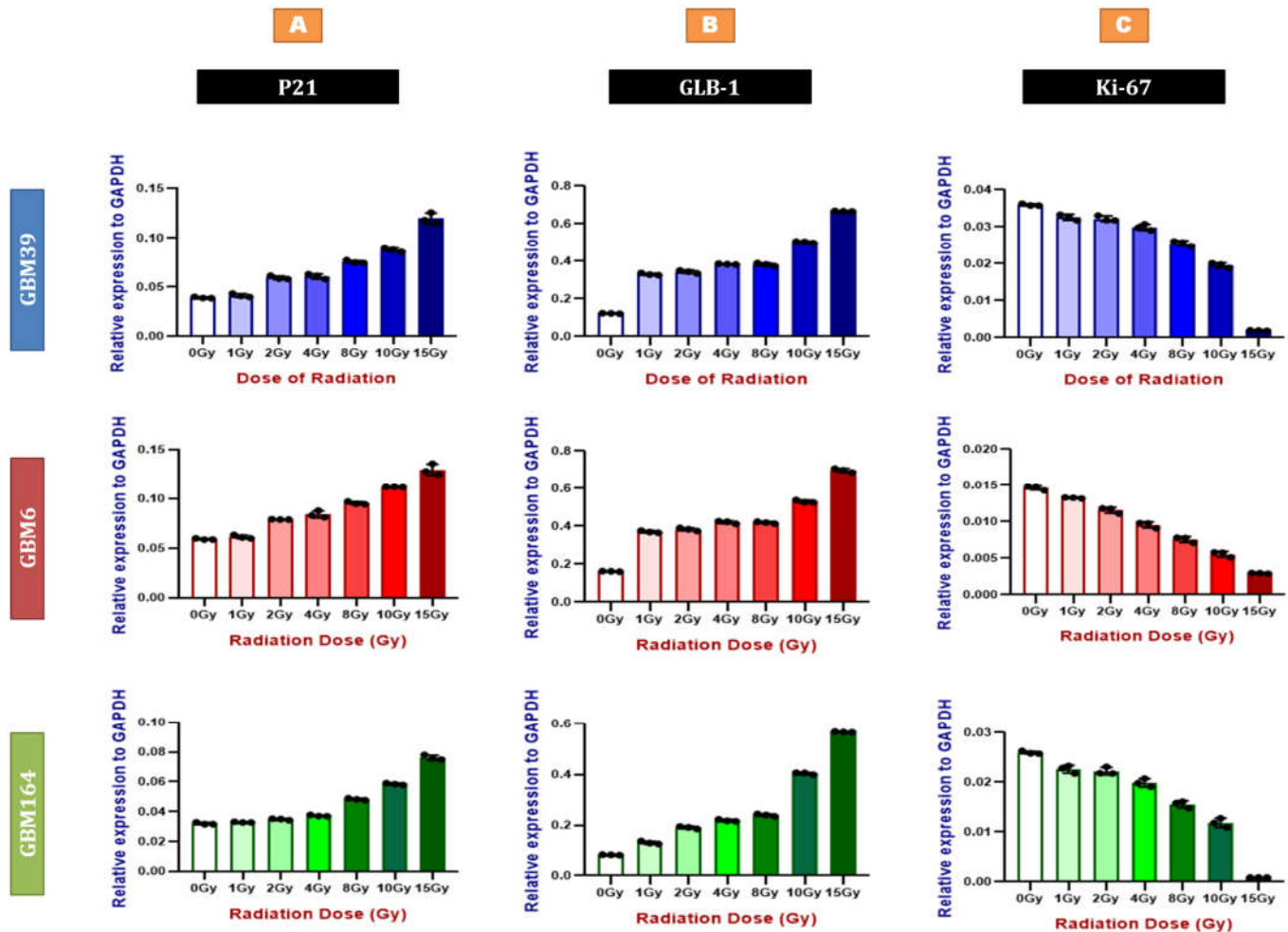


Figure 1. Radiation induces senescent-like gene expression in a dose-dependent manner. qRT-PCR for P21 (A), GLB-1 (B), and ki-67 (C) using RNA extracted from GBM39 (Blue), GBM6 (Red), and GBM164 (Green) cells after different doses of irradiation as shown in the Materials and Methods compared to the sham (0Gy) irradiated group. Y axes demonstrate expression relative to the house-keeping gene, GAPDH. Individual data points are shown, representing a biological triplicate of 3 independent experiments. Each data point represents a mean of a technical triplicate. Error bars represent SD between the independent experiments.

2.2. P21 overexpression inhibits human GBM proliferation and promotes cellular senescence

To functionally determine how P21 expression impacts measures of senescence and viability in glioma cells, we utilized CRISPR-based gain and loss of function strategies to modulate P21 expression. We utilized CRISPR/dCas-VPR and CRISPR/Cas9 technology to overexpress and delete P21, respectively, in each cell line using non-targeting sgRNA sequences as controls for each experiment. Cells were evaluated after genetic modification for cell viability and gene expression. The resultant decline and gain of P21 expression were evaluated by qPCR (Figure 2A). In each line, P21 deficient cultures (Figure 2B) yielded significantly higher viability, while P21-overexpressing cells showed lower viability as evaluated via an ATP-mediated luminescent assay. This correlated with a significant increase in ki-67 expression and decreased expression of GLB-1 levels with P21 loss, while the opposite was true with P21 overexpression (Figure 2C, D). Collectively, these data suggested P21 may act through both regulation of both cell proliferation and viability.

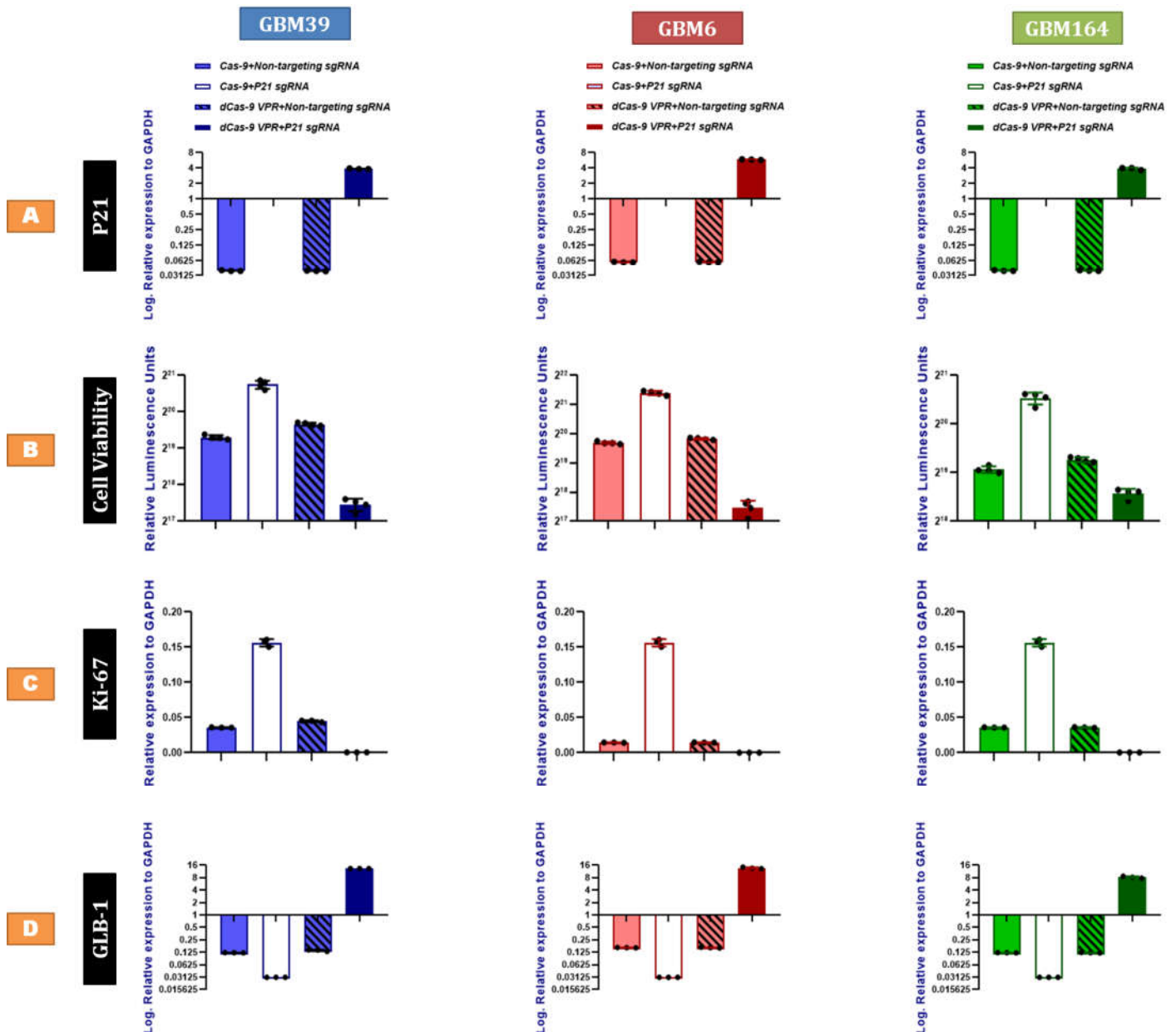


Figure 2. P21 overexpression inhibits human GBM proliferation and promotes cellular senescence. (A) qRT-PCR for P21 confirming the gene editing (knock-out using CRISPR/Cas9 and knock-in using dCas9-VPR) compared to the corresponding controls treated with non-targeting sgRNAs, using RNA extracted from GBM cells as shown including GBM39 (Blue), GBM6 (Red), and GBM164 (Green). Y axes (A, C, D) demonstrate log expression relative to the house-keeping gene, GAPDH. (B) Cell titer-glo assay demonstrating the cell viability of GBM cells in response to the knock-out vs. the knock-in of P21, compared to the same cells treated with a scrambled non-targeting sgRNAs. (C) qRT-PCR for ki-67 in the P21-genetically modified cells (P21 knock-in vs. P21 knock-out) compared to the corresponding controls treated with non-targeting sgRNAs. (D) qRT-PCR for GLB-1 in the P21-genetically modified cells (P21 knock-in vs. P21 knock-out) compared to the corresponding controls treated with non-targeting sgRNAs. Results were obtained from three independent experiments. Each data point represents the mean of technical triplicates. Error bars represent SD between the independent experiments, * p value <0.0001.

2.3. P21 overexpression induces tumor cell apoptosis by activating the p53-upregulated modulator of apoptosis

The inverse correlation between ATP level and P21 expression could reflect more rapid proliferation in the P21-deficient cells, however, the early timepoint of analysis after genetic alteration make this unlikely to be the sole explanation. As such, we also asked if

P21 activity could also directly impact cell viability, independent of cell proliferation, via evaluation of caspase 3 activity. Indeed, P21 overexpression increased caspase-3 enzymatic activity suggesting that P21 induction directly promotes apoptosis (**Figure 3A**). The critical role of P21 in cellular senescence is well recognized. Our prior work suggested that PUMA (p53-upregulated modulator of apoptosis) promotes apoptosis in senescent glioma cells, but is countered by Bcl-xL to enable survival. Similarly, we found increased PUMA expression in each line of P21-overexpressing human GBM (**Figure 3B**), which likely facilitates apoptosis in response to P21 overexpression. Further, SNAI (SLUG), a well-known biological inhibitor of PUMA and p53 [22], was significantly decreased in P21-overexpressing cells for each GBM line, positioning SNAI as a plausible regulator of P21-mediated PUMA expression.

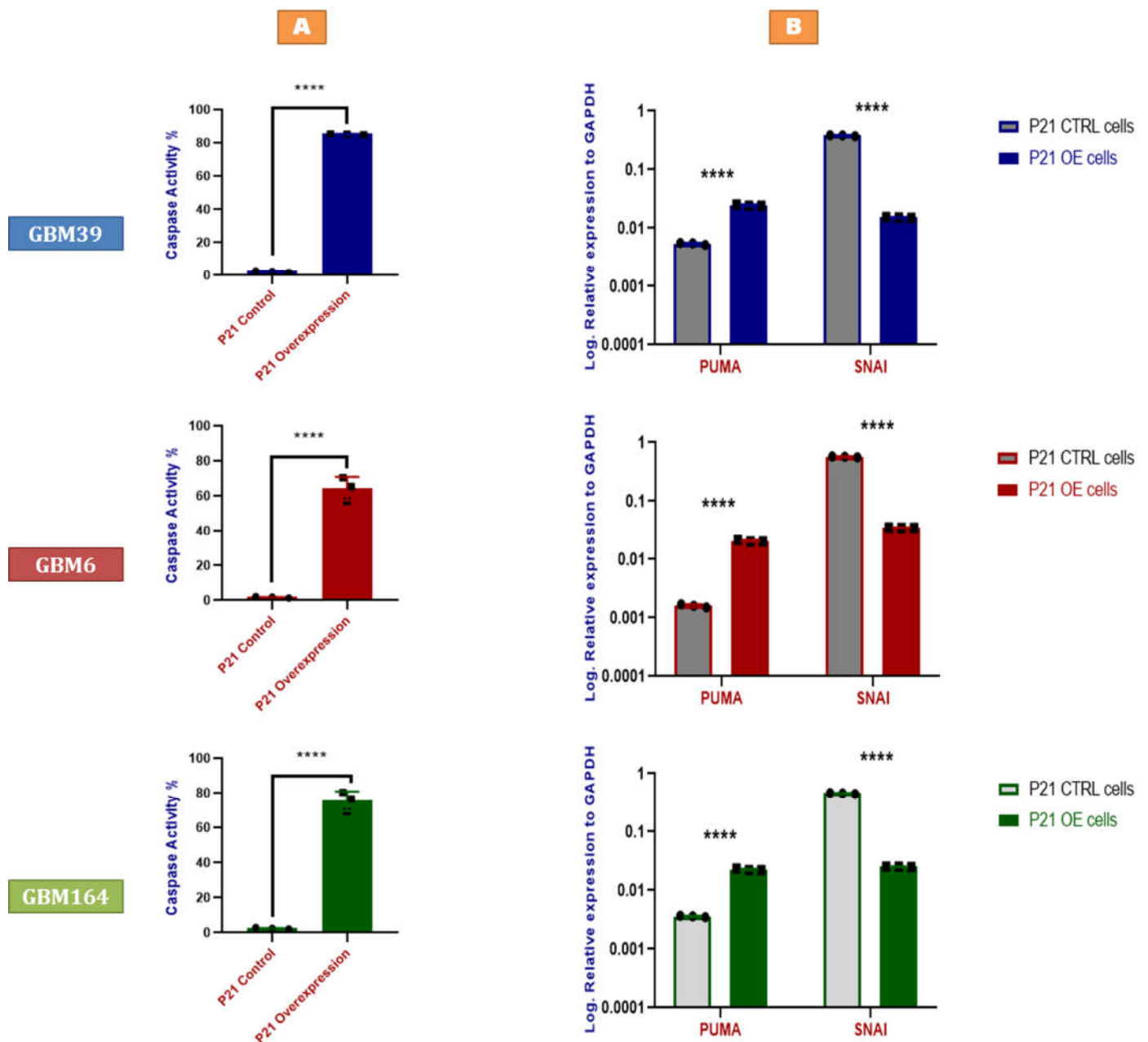


Figure 3. P21 overexpression induces tumor cell apoptosis by activating the p53-upregulated modulator of apoptosis. (A) Fluorescence-based caspase assay indicating caspase-3 enzymatic activity in GBM39 (Blue), GBM6 (Red), and GBM164 (Green) cells in response to P21 knock-in (overexpression). Values are normalized to results acquired from the same cell lines treated with scrambled non-targeting sgRNAs. Error bars represent SD from three different samples (biological triplicates),

as indicated by the individually plotted data points. Each data point represents the mean of three technical replicates. A summary of the p value is shown. **(B)** qRT-PCR for PUMA and SNAI (SLUG) in P21-overexpressing (knock-in) cells compared to the corresponding control cells treated with a non-targeting scrambled sgRNA, using RNA extracted from GBM39 (**Blue**), GBM6 (**Red**), and GBM164 (**Green**) cells. Y axes demonstrate log expression relative to the house-keeping gene, GAPDH. Individual data points are shown, representing a biological triplicate of 3 independent experiments. Each data point represents a mean of a technical triplicate. Error bars represent SD between the independent experiments, p values <0.0001. A summary of the p value is shown.

2.4. P21-mediated senescence in GBM cells

Since some cells survived direct P21 overexpression, we sought to further characterize these surviving cells. Our earlier experiments (Figure 2 C, D) demonstrated decreased proliferation and GLB-1 in P21-overexpressing cells, suggestive of senescence. As such, we asked if such cells also demonstrate histologic features of senescence, including enzymatic beta-galactosidase (beta-gal) activity and expression of Senescence Associated Secretory Profile (SASP) [16,17]. P21-deleted cells demonstrated no significant change in the baseline low percentage of cells with beta galactosidase staining, though all three lines showed markedly increased beta-gal staining upon P21 overexpression (**Figure 4A**). Further consistent with a senescent phenotype, we also observed increased expression of the SASP factors transforming growth factor beta (TGF- β), and interleukin 6 (IL-6), beta galactosidase (GLB-1), along with a marked drop in the nuclear protein (ki-67) in P21-overexpressing cells, while opposite findings were detected in P21-deleted cells (**Figure 4B**).

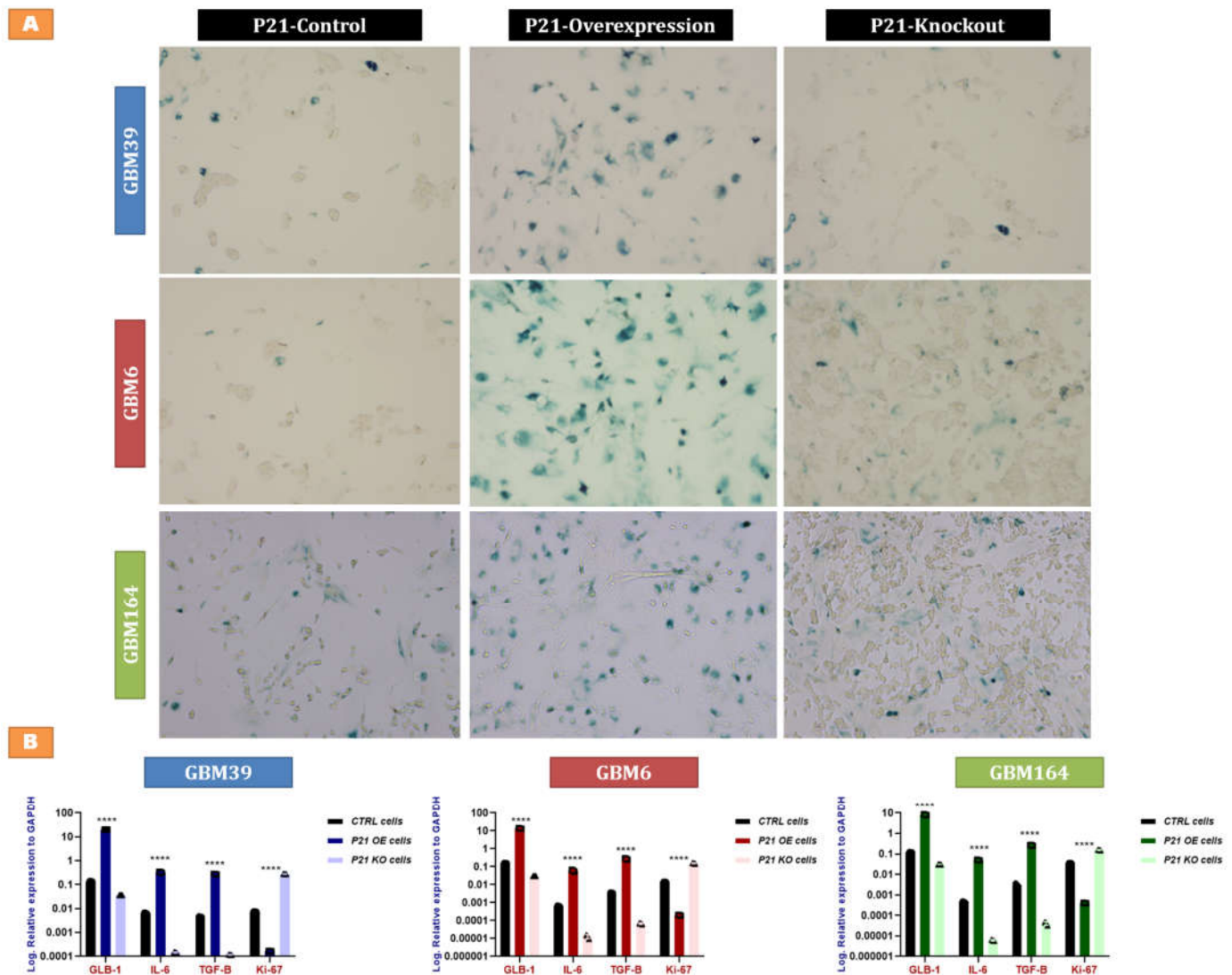


Figure 4. P21-mediated senescence in GBM cells. (A) Senescence-associated beta-galactosidase staining in the P21-genetically modified (P21 knock-in vs. P21 knock-out) GBM39 (Blue), GBM6 (Red), and GBM164 (Green) cells, compared to the corresponding control cells treated with non-targeting sgRNAs. (B) qRT-PCR for GLB-1, IL-6, TGF-B, and Ki-67 in the P21-genetically modified cells (P21 knock-in vs. P21 knock-out) compared to the corresponding control cells treated with non-targeting sgRNAs using RNA extracted from GBM39 (Blue), GBM6 (Red), and GBM164 (Green) cells. Y axes demonstrate log expression relative to the house-keeping gene, GAPDH. Individual data points are shown, representing a biological triplicate of 3 independent experiments. Each data point represents a mean of a technical triplicate. Error bars represent SD between the independent experiments, p values <0.0001. A summary of the p value is shown.

2.5. Faster and more stable senescence with P21 overexpression, than irradiation.

Senescence can be induced by DNA damaging agents including radiation which is one of the standard therapies against glioblastoma. Unfortunately, glioblastoma escapes senescence as evidenced via inevitable recurrence [18]. To assess the relative impacts of radiation-versus P21 overexpression-induced senescence, we treated each of the three cell lines with P21 versus 15Gy radiation, which induces senescence in human glioblastoma cells [18]. Interestingly, we observed a more rapid elevation and a stable maintenance of GLB-1 levels in P21-overexpressing cells compared to irradiation-treated cells, wherein GLB-1 induction was less robust and started to decline after 21days (Figure 5A).

2.6. P21-induced senescence relies on Bcl-xL for survival

We have previously shown that chemotherapy and radiation-induced GBM cells escape apoptosis via the anti-apoptotic actions of Bcl-xL. We asked if Bcl-xL could also be relevant to cell survival in the context of direct P21-induced senescence. At 7 days after P21 overexpression, we observed upregulation of multiple anti-apoptotic proteins including BCL-2, Bcl-xL and MCL-1 (**Figure 5B**). The fold-change from baseline in these cells was greatest for Bcl-xL, suggesting a potentially increased dependency of these human glioma cells upon Bcl-xL after P21 exposure.

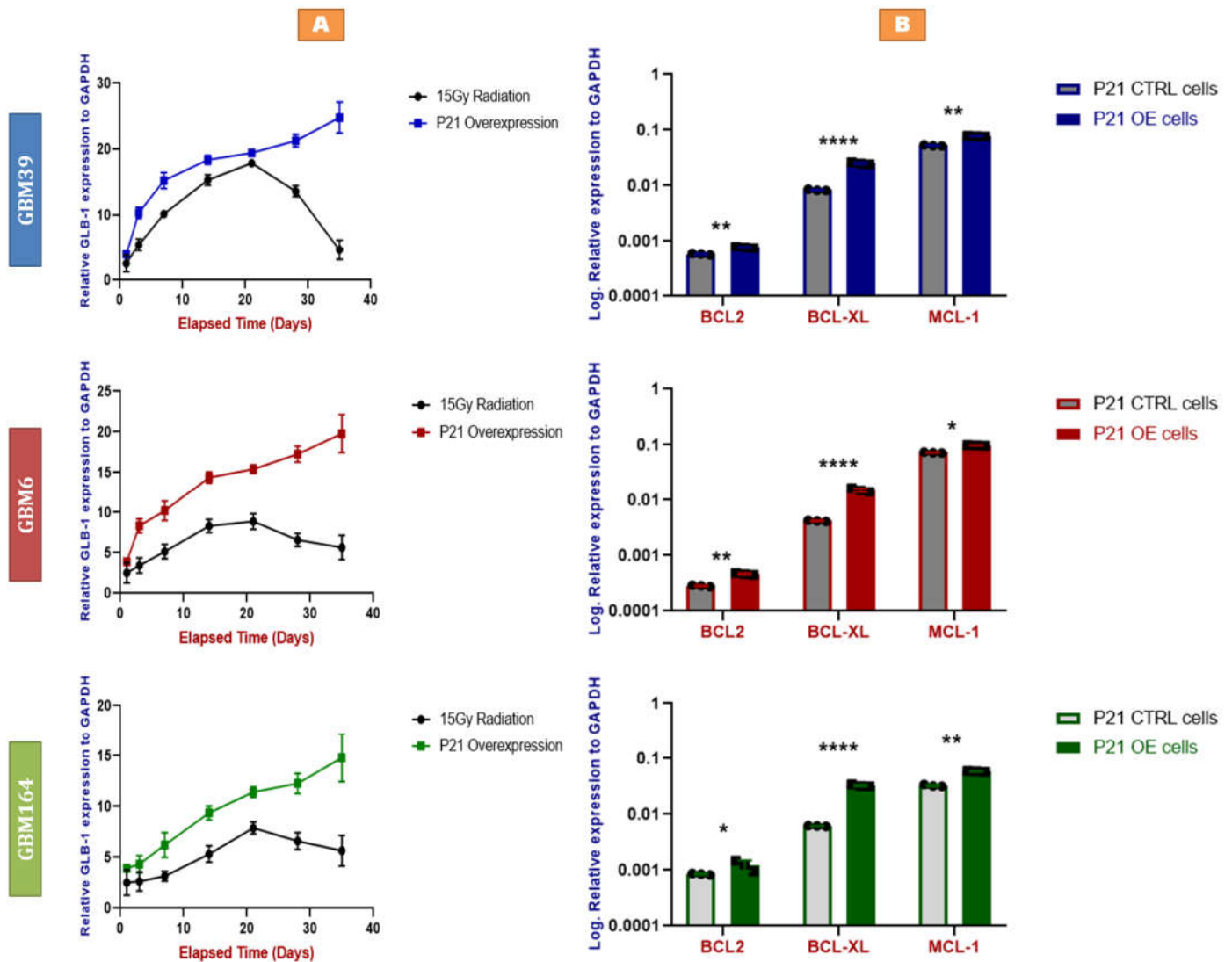


Figure 5. (A) Faster and more stable senescence with P21 overexpression, than irradiation. qRT-PCR for GLB-1 in the P21-overexpressing (knock-in) cells compared 15Gy-irradiated cells, using RNA extracted from GBM39 (Blue), GBM6 (Red), and GBM164 (Green) cells at different times points (1, 3, 7, 14, 21, 28, and 35days). Y axes demonstrate log expression relative to the house-keeping gene, GAPDH. Individual data points are shown, each data point represents a biological triplicate of 3 independent experiments. Error bars represent SD between the independent experiments (biological triplicate). (B) P21-induced senescence relies on Bcl-xL for survival. qRT-PCR for BCL2, Bcl-xL, and MCL-1 in P21-overexpressing (knock-in) cells compared to the corresponding control cells treated with a non-targeting scrambled sgRNA, using RNA extracted from GBM39 (Blue), GBM6 (Red), and GBM164 (Green) cells. Y axes demonstrate log expression relative to the house-keeping gene, GAPDH. Individual data points are shown, representing a biological triplicate of 3 independent experiments. Each data point represents a mean of a technical triplicate. Error bars represent SD between the independent experiments. A summary of the p values is shown.

2.7. Bcl-xL knock-down induces apoptosis in P21-induced senescent glioblastoma cells

Based on these data, we used shRNAs targeting Bcl-xL, BCL-2 and MCL-1 anti-apoptotic proteins in stably P21-overexpressing senescent glioblastoma cells as compared to naïve cells or cells deficient for P21. By 3 days after Bcl2, Bcl-xL or Mcl-1 knockdown, we observed a significant drop in cell viability P21-overexpressing, with most marked decline in cells receiving the Bcl-xL knockdown. These data are similar to our prior findings of Bcl-xL dependency in TMZ- and radiation-induced senescent GBM cells, and could suggest that-induced Bcl-xL dependency is mediated through P21. (Figure 6A). Consistent with our previously reported pro-apoptotic mechanism of PUMA-mediated cell death upon Bcl-xL blockade (ref, or reference to figure), we also detected a significant increase in Caspase-3 enzymatic activity in each cell line in response to Bcl-xL knock-down (Figure 6B). Conversely, applying these shRNAs to P21-control or P21-overexpressing glioblastoma cells yielded relatively minimal impact on cell viability (Figure 6).

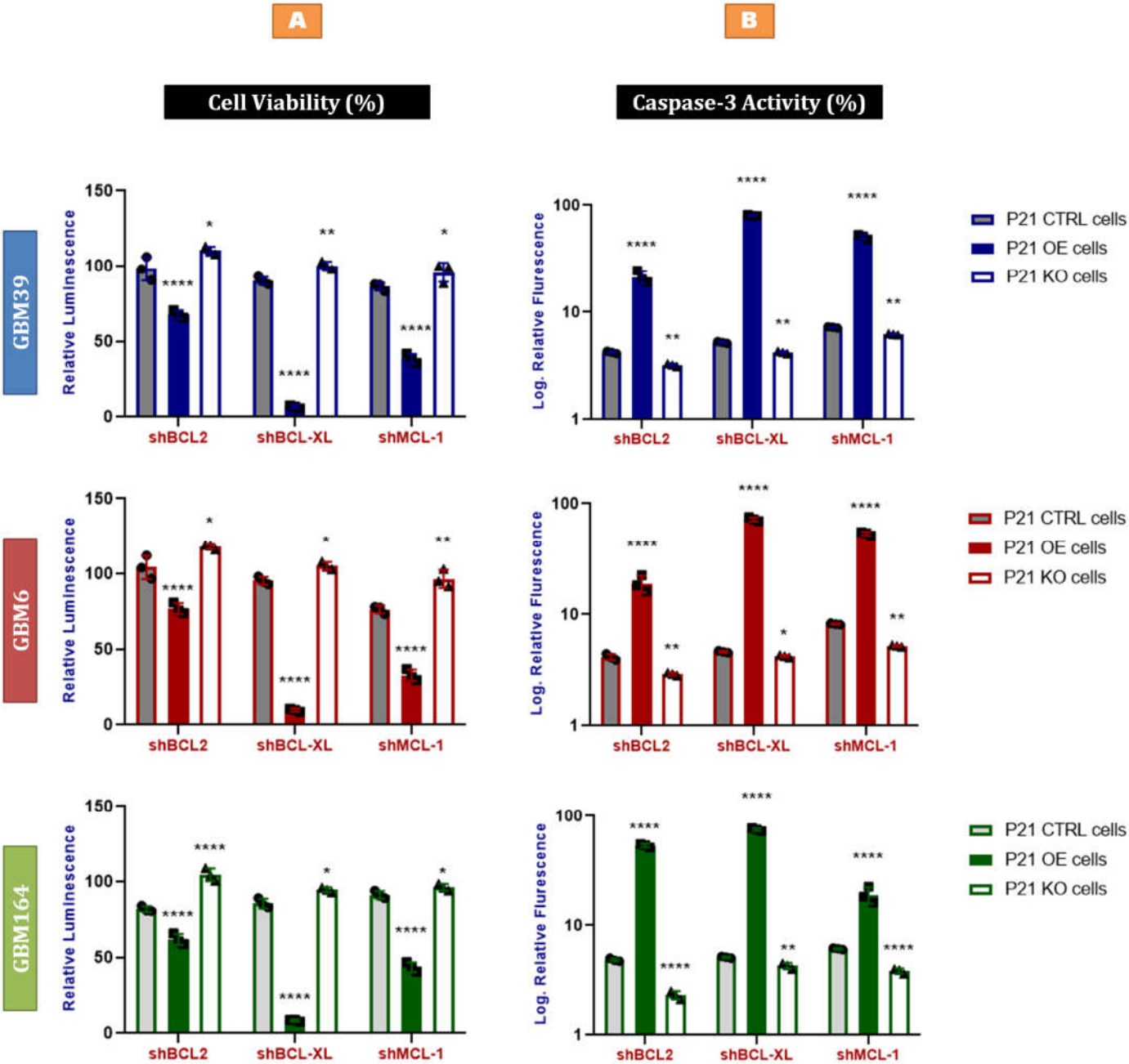


Figure 6. Bcl-xL knock-down induces apoptosis in P21-induced senescent glioblastoma cells (A) Cell titer-glo assay demonstrating the cell viability of GBM39 (Blue), GBM6 (Red), and GBM164 (Green) P21-genetically modified cells (knock-in and knock-out) compared to the corresponding control cells, in response to the knock-down of BCL2, Bcl-xL, and MCL-1 using shBCL2, shBcl-xL, and shMCL-1 vectors. Error bars represent SD values from three different samples (biological triplicates) of each cell line, as indicated by the individually plotted data points. Each data point represents the mean of three technical replicates. A summary of p values is shown. (B) Fluorescence-based caspase assay demonstrating the caspase-3 activity in GBM39 (Blue), GBM6 (Red), and GBM164 (Green) P21-genetically modified cells (knock-in and knock-out) compared to the corresponding control cells, in response to the knock-down of BCL2, Bcl-xL, and MCL-1 using shBCL2, shBcl-xL, and shMCL-1 vectors. Error bars represent SD values from three different samples (biological triplicates) of each cell line, as indicated by the individually plotted data points. Each data point represents the mean of three technical replicates. A summary of p values is shown.

3. Methods

3.1. Cell culture and growth conditions:

GBM6, GBM39, and GBM164 human glioblastoma cell lines were obtained from the National (Patient-Derived Xenografts) PDX resource [38]. All cell lines were cultured and maintained in antibiotic-free FBS media, composed of 10% Fetal Bovine Serum (FBS) and 90% Dulbecco's Modified Eagle's medium (DMEM). Cells were passaged regularly once they reached 70-90% confluence using phosphate-buffered saline (PBS) and 1X Trypsin-EDTA (0.05% Trypsin and 0.53mM EDTA). All experiments were performed using 3rd passage cultured cells.

3.2. Irradiation of cells:

1-3X10⁶ GBM cells were plated either in 10cm or 7cm sterile tissue culture vessels and maintained in culture for 2-3 days until they become 50-60% confluent then exposed to cesium γ -radiation (1, 2, 4, 8, 10, or 15Gy).

3.2. Cell viability assay:

The number of viable cells in culture was measured using the Cell Titer-Glo® Luminescent Cell Viability Assay as per the manufacturer's instructions and protocol (Promega, G7570, G7571, G7572, and G7573). The Cell Titer-Glo® Luminescent Cell Viability Assay is a method to determine the number of viable cells in culture based on quantification of ATP to detect metabolically active cells.

3.3. Caspase-3 assay:

Caspase-3 enzymatic activity was measured in cell lysates prepared from GBM cell lines using a Caspase-3 Activity Assay Kit (Cell Signaling Technology, #5723) as per the manufacturer's instructions. The Caspase-3 Activity Assay Kit is a fluorescent assay that detects caspase-3 in cell lysates. It contains a fluorogenic substrate (N-Acetyl-Asp-Glu-Val-Asp-7-amino-4-methylcoumarin or Ac-DEVD-AMC) for caspase-3. During the assay, activated caspase-3 cleaves this substrate between DEVD and AMC, generating highly fluorescent AMC that can be detected using a fluorescence reader with excitation at 380 nm and emission between 420 - 460 nm. Cleavage of the substrate only occurs in lysates of apoptotic cells. Therefore, the amount of AMC produced is proportional to the number of apoptotic cells in the sample.

3.4. Quantitative real-time PCR (qRT-PCR):

RNA was extracted from GBM cells as the following, cells were washed with PBS before being homogenized with TriZol reagent (Invitrogen). RNA precipitation was performed at -20C overnight (12-18 hours). The precipitated RNA pellets were dissolved in RNase-free water and concentration was measured by absorbance at 260 nm (A260) using Nanodrop2000. cDNA synthesis was performed with 1 μ g of total RNA using a M-MLV reverse transcriptase kit (ThermoFisher, # 28025013 and 28025021) as per the

manufacturer's protocol. 25ng of cDNA was used for real-time PCR by Taqman gene expression assay targeting the gene of interest on an ABI 7500/7500-Fast Real-Time PCR System (Applied Bioscience). The relative expression of each gene was determined by the $\Delta\Delta CT$ method.

3.5. Viral packaging and gene knock-down by shRNA:

Plasmid sequences for shRNAs were either designed manually using commercially available software or purchased as already designed sequences from Addgene. The sequence was provided in the form of a bacterial plasmid. Bacteria were cultured in Lysogeny broth (LB) media and Ampicillin (to kill any intervening bacteria without the plasmid of interest). A single bacterial colony was selected from the bacterial culture and further expanded. Plasmid DNA from the bacteria was isolated and purified using a PureLink™ HiPure Plasmid Miniprep kit (Invitrogen, #K210002 and K210003) as per the manufacturer's protocol. Isolated DNA concentration and purification were measured using NanoDrop (ThermoFischer). Viral packaging was performed as per the manufacturer's (Addgene) protocol using 10µg of DNA plasmid to transfect 3.8×10^6 HEK293 cells in a 10cm tissue culture dish. The virus was harvested 72 hours post-transfection. Viral supernatant was centrifuged at 500g for 5 minutes to pellet any packaging cells that were collected during harvesting. The supernatant was filtered through a 0.45µm polyethersulfone (PES) filter. Viral supernatant was aliquoted and snap-frozen in liquid nitrogen and stored at -80C to avoid loss until time transduction was performed. $5-8 \times 10^5$ GBM cells were plated in 6-well plates and incubated at 37C overnight (16-18hours). The following day, 10-20µl of viral supernatant were added to each well and incubated at 37C for 36-72 hours. The protein then was extracted to confirm knock-down and cells were re-plated for any further experiments.

3.6. Gene knock-out by CRISPR/Cas9:

Plasmids encoding for Cas9 protein were purchased from the Addgene online service along with plasmids encoding for Puromycin-resistance gene. Provided bacterial plasmids were cultured in Lysogeny broth (LB) media and Ampicillin. A single bacterial colony was selected from the bacterial culture and further expanded. DNA Plasmid from the bacteria was isolated and purified using a PureLink™ HiPure Plasmid Miniprep kit (Invitrogen, #K210002 and K210003) as per the manufacturer's protocol. Isolated DNA concentration and purification were assayed using NanoDrop. Viral packaging was performed as described in the viral packaging section. GBM cells were cultured in a 6-well plate at a density of $5-8 \times 10^5$ cells in 2ml of antibiotic-free media/ well. Cells were incubated overnight (16-18 hours) at 37C. The following day, 10-20µl of viral supernatant were added to each well and incubated at 37C for 48-72 hours. Transduced cells then were treated with Puromycin for 48 hours to ablate all non-transduced cells. Surviving cells were expanded in culture. The presence of Cas9 in the cells was verified by Western blot using a Guide-it Cas9 polyclonal antibody (TaKaRa, Cat. Nos. 632606 & 632607). Viral vector encoding for P21 was generated using the same way as described above. Cas9 gene editing activity and the success of CRISPR knock-out were checked using a Guide-it Mutation Detection kit (TaKaRa, Cat. No. 631448). Then another step of confirmation by qRT-PCR and western blotting. By using qRT-PCR, knocked-out P21 was not detectible, even at high RNA concentrations, confirming the success of CRISPR/Cas9 knock-out.

3.7. Gene knock-in (overexpression) by dCas-VPR:

The protocol can be divided into 2 parts:

3.7.1. Generating cell lines that constitutively express dCas9-VPR

GBM cells were plated overnight in six-well plate with the optimum cell density of 8×10^5 cells per well in reduced-serum medium (Optimum Medium). The following day, cells were transduced with lentiviral particles carrying dead or deactivated cas9 (dCas9)

fused with one or more transcriptional activators (dCas9-VPR) along with Blasticidin resistance marker (BlastR) (Dharmacon), the transduction done with a mode of infection (MOI) equals to .3TU/cell. On the third day post transduction, media was changed and replaced with selection media containing blasticidin antibiotic (Selection media). Selection media was replaced after 2 days with antibiotic-free media. Cells were kept in the antibiotic-free media for expansion, while few cells were harvested from the culture to confirm the expression of dCas9-VPR in these cells by western blotting.

3.7.2. Inducing P21 overexpression

dCas9-expressing GBM cells were plated overnight in six-well plate with a cellular density of 4×10^5 cells per well. On the following day, 10-20ul of viral supernatant encoding for P21 was added to each well of the six-well plate. 2 days post transduction; few cells were used for RNA extraction to confirm the gene overexpression by qRT-PCR. N.B; the number of cells and the viral supernatant volume mentioned above, was optimized by us after several trials to ensure that all the cells will overexpress P21. We do not recommend any volume change if the same cells are used.

3.8. Senescence-associated β -galactosidase staining:

Senescence-associated β -galactosidase staining Kit (Cell Signaling Technology #9860) was used as an indicator of relative senescence after radiation as per the manufacturer's directions. Briefly, cells were fixed for 10 min in β -galactosidase fixative Solution (10% 100x Fixative Solution; 90% H₂O), and washed with PBS. The cells were then stained with β -Galactosidase Staining Solution (93% 1x Staining Solution; 1% 100x Solution A, 1% 100x Solution B, 5% X-gal. Wells without samples were filled with PBS, and the plate was wrapped in parafilm to prevent evaporation. The plate was left overnight in a dry incubator at 37°C. The next day, cells were examined under a microscope for β -gal-positive cells (blue staining). PBS was added to the wells, and the plate was placed on the rocker (speed = 30/min) for 5 minutes. The plate was washed three times. Staining was performed in sham and vehicle-treated control, 10Gy, 15Gy radiated, and TMZ treated GBM39 cells. To see the senescence maturation over time, Beta-Gal staining performed at day 0, 7, and 14 following 15Gy radiation. For each time points and conditions staining done at multiple wells.

3.9. Statistical analysis

All experiments were repeated at least three times. Statistical analysis was performed with one-way ANOVA and unpaired 2-tailed t-test using GraphPad prism 8.4.2. Error bars represent the SD values and significance was taken as $p < 0.05$, $p^{**} < 0.01$, $p^{***} < 0.001$, $p^{****} < 0.0001$. Unless otherwise stated, each data point reflects the average of three technical replicates. Error bars show standard deviation of biological replicates.

3.10. Reagents and antibodies:

Reagent	Manufacturer	Catalogue Number
DMEM (Dulbecco's Modified Eagle's Medium)	Corning	10-013-CV
Trypsin EDTA 1X	Corning	25-052-CI
Opti-MEM™ I Reduced Serum Medium	Gibco	31-985-070
Blasticidin S HCl	ThermoFischer	A1113903
Puromycin Dihydrochloride	ThermoFischer	A1113803
Guide-it Cas9 Polyclonal Antibody	TaKaRa	632606 & 632607
Guide-it Mutation Detection kit	TaKaRa	631448
PureLink™ HiPure Plasmid Miniprep kit	Invitrogen	K210002 and K210003
LB Broth	Gibco	10855021
M-MLV reverse transcriptase kit	ThermoFisher	28025013 and 28025021
The Cell Titer-Glo®	Promega	G7570, G7571, G7572, and G7573
Caspase-3 Activity Assay Kit	Cell Signaling Technology (CST)	5723
TRIzol™ Reagent	Invitrogen	15596018

***Designed sequences for primers, shRNAs, and sgRNAs that are used in this study, are provided with detailed information as a part of the raw data.

4. Discussion

Recent studies showed that surviving cancer cells with an initially senescent phenotype following chemoradiation, were able to escape senescence over time, giving rise to tumor cells that were more aggressive and resilient than those present in the original tumor [23,24]. Therefore, more powerful approaches are needed to either keep these glioma initiating cells in senescent state for longer, or to eliminate these senescent cells prior to tumor recurrence.

In our current study, we demonstrate that P21 is a potentially powerful mediator of cell fate, able to single-handedly replicate or exceed the pro-apoptotic and senescence-inducing impacts of high-dose radiation.

P21 is a potent cell cycle inhibitor, which binds and inhibits several cyclins and cyclin-dependent kinases, such as CDK2, -CDK1, and -CDK4/6 complexes [13,14]. Cells with high P21 typically enter a G0/quiescent state, whilst those with low P21 continue to proliferate [25]. Since P21 is downstream to p53 which is frequently mutated in cancer, P21 activity can be dysregulated in cancer. Indeed, some studies have suggested that P21 can paradoxically promote proliferation in cancer cells under certain conditions [26,27,28,29,30]. We directly manipulated P21 in both P53-mutant (GBM6) and P53-WT cells with (GBM164) and without (GBM39) IDH-mutation and observed that P21-induced apoptosis and senescence in surviving cells in each cell line.

P53 regulates both apoptosis and senescence. P21 is downstream of P53 and considered a master regulator of senescence, while other mechanisms are thought to regulate P53-mediated apoptosis. As such, the robust finding of direct P21-mediated upregulation of apoptosis was unexpected. The pro-apoptotic gene PUMA is considered downstream of P53 rather than P21, though P53-independent regulation is well documented. Of note, PUMA and P53 transcription are both negatively regulated by SLUG, which was also downregulated in the P21 overexpressing cells and may help explain the observed PUMA upregulation in P21-overexpressing cells [22]. That PUMA was induced by P21 overexpression in GBM6 which lacks functional P53 suggests that P21 is sufficient to directly regulate SNAI/PUMA to impact cell survival in a P53-independent manner.

P21-induced senescence is consistent with prior reports. However, its powerful and lasting impact in GBM cells raises questions if P53-independent mechanisms could be utilized to leverage its anti-tumorigenic potential. Our data suggest that, if possible, leveraging P21 directly could help circumvent arguably the most common mechanism of cancer cell survival, P53 mutation, without compromising cellular ability to induce apoptosis or maintain senescence. Further studies in a broader array of P53-mutant cells will be

necessary to determine whether or not this concept could be more widely generalizable. Moreover, *in vivo* studies would be needed to determine if the pro-apoptotic and antiproliferative impacts of P21 induction we observe *in vitro* could translate into a survival advantage. If so, pharmacologic efforts aimed at direct P21 induction within cancer cells could provide a novel strategy for cancer control.

Although P21 overexpression induced cell death in a large percentage of glioma cells, some cells were able to survive as is typical of cancer cells in response to almost any cancer therapy. However, upon examining these cells microscopically, we found that these cells started to exhibit characteristic morphological features such as the increased size, new irregular shapes, a darker nucleus, cytoplasmic vacuolation, and other features which are characteristic to senescent cells [31]. To confirm that these glioma cells are indeed senescent, we used a senescence-associated beta-galactosidase stain and qPCR which supported the presence of senescence in these glioma cells. Moreover, rigorous definitions of senescent cells include evidence of SASP (senescence associated secretory profile/phenotype), wherein those cells secrete high levels of immunoregulatory cytokines and proteases [32,33]. Both common SASP factors, IL-6 and TGF- β , used to screen for SASP revealed significant upregulation in all cells consistent with a senescent phenotype. Curiously and excitingly, direct P21 overexpression appeared to lead to a senescent phenotype that was induced more rapidly, intensely, and in a more lasting manner as compared to radiation as evaluated via GLB-1 expression (Fig 5B). SASP may also consist of exosomes and ectosomes containing enzymes, microRNA, DNA fragments, chemokines, and other bioactive factors [34,35]. Initially, SASP is immunosuppressive (characterized by transforming growth factor beta, TGF- β) and pro-fibrotic, but progresses to become proinflammatory (characterized by IL-1 β , IL-6 and IL-8) and fibrolytic [36,37]. Therefore, we screened these glioma cells for SASP factors such as TGF- β and IL-6 to confirm the positive results we got from the beta galactosidase stain, and indeed we were able to detect higher levels of these inflammatory markers in glioma cells tested positive for beta-galactosidase staining, further confirming that these glioma cells are senescent indeed.

At this point, we were able to confirm that our new approach of inducing senescence in glioma cells was effective, but standard irradiation can induce senescence in glioma cells as well, so which method is more effective in inducing and maintaining senescence in glioma cells?! and by which method can glioma cells stay quiescent for a longer period of time, the current standard method of irradiation or our p21-based method?!

In order to provide a scientific answer to this question, we established two groups of senescence across several lines of glioma cells. The first group, was treated with a high dose of irradiation (15Gy) which is reported to be more than enough in inducing senescence in glioma cells [18], and we started following these cells from as early as 24hrs after irradiation with the senescence-specific beta galactosidase (GLB-1) mRNA levels. At the same time, we started following the second group of cells which was treated with p21-overexpressing vector, using the same GLB-1. Surprisingly, we identified three advantages of p21-induced senescence over irradiation-induced senescence. The first one was that GLB-1 levels started to go up significantly from as early as 72hrs in p21-overexpressing cells compared to irradiation-treated cells which took them longer to significantly upregulate GLB-1 levels (~7days). The second advantage observed, was that GLB-1 uppermost value in irradiation-treated cells was detected at about 21days, but it was far behind the corresponding value in p21-overexpressing cells at the same time, especially in GBM6 and GBM164. The third and the most important advantage observed, was that in irradiation-treated cells, the GLB-1 levels started to decrease after reaching its maximum value at 21days, in contrast to the corresponding values in p21-overexpressing cells which surprisingly continues to gradually increase over time, the finding that encouraged us to start a broad range of In-vivo and ex-vivo studies which are currently in progress.

Although at this point, we had confirmed that our new approach could be better than the standard irradiation method in inducing cellular senescence in human glioma cells and keeping these cells quiescent for a longer period of time, we were interested in investigating the potential mechanisms that keep these senescent cells alive. Our rationale was

that if we could identify the survival mechanisms that keep these senescent glioma cells alive, we can come up with interventions that target and kill these cells to deprive them from any hope of escaping senescence at any later time because simply they will not be existing anymore. Our prior work demonstrated that senescent glioma cells are selectively dependent upon Bcl-XL, as compared to non-senescent cells [18]. Similarly, P21 overexpressing cells were relatively more vulnerable to Caspase-3-mediated apoptosis following depletion of Bcl-XL than Bcl-2 or Mcl-1 (Fig 6A)—consistent with more prominent upregulation of Bcl-XL than Bcl-2 or Mcl-1 following P21 overexpression (Fig 5B). Based on that, we started examining these p21-induced senescent glioma cells, looking for multiple anti-apoptotic proteins, such as Bcl-xL, Bcl-2, and MCL-1. We found that these p21-induced senescent glioma cells upregulated three anti-apoptotic proteins (Bcl-xL, Bcl-2, and MCL-1), but the significant upregulation was of the share of Bcl-xL. For a further confirmation and as a potential application for such a finding, we used shRNAs to target Bcl-xL, Bcl-2, and MCL-1 in these senescent glioma cells. In response to the knock-down, a decrease in the cell viability along with an increase in the caspase activity were observed and detected in these senescent glioma cells, but the significant results were achieved in response to Bcl-xL knock-down in a particular, confirming the previous finding of the dependency of p21-induced senescent glioma cells on Bcl-xL, and suggesting a potential target to eliminate these senescent glioma cells and prevent their recurrence.

Collectively, these findings demonstrate that P21 is a powerful mediator of glioma cell fate which promotes desirable outcomes of prolonged sustained senescence or apoptosis. Exploring potential avenues to directly upregulate P21 could provide novel opportunities to improve outcomes for glioma.

Supplementary Materials: Figure S1. An existing correlation between P21 and senescence in human glioblastoma. qRT-PCR for P21.

Author Contributions: Project conception: TCB, MAM; Experimental design: MAM, TCB; Contributed cell lines, reagents or protocols: AEW, MR, AAA; Performed experiments: MAM, MR; Statistical analysis: MAM, TCB, AAA; Wrote the Manuscript: MAM, TCB; Diagrams and Illustrations design: MAM; Critical review, feedback and final approval: All Authors.

Funding: This work was supported by NINDS (NRCDP), NS109770, the NIA (R37 AG013925, and P01AG062413), Mayo Clinic Cancer Center, Center for Individualized Medicine, and Robert and Arlene Kogod Center on Aging, Brains Together for the Cure, Humor to fight the Tumor, Lucius & Terrie McKelvey, the Connor Fund, Robert P. & Arlene R. Kogod, Robert J. & Theresa W. Ryan, and the Noaber Foundation.

Conflicts of Interests: Patents on senolytic drugs and their uses are held by Mayo Clinic. This research has been reviewed by the Mayo Clinic Conflict of Interest Review Board and was conducted in compliance with Mayo Clinic Conflict of Interest policies.

Data Availability Statement: Data supporting the findings of this study are available on request from the corresponding authors.

References

1. Partridge L, Deelen J, Slagboom PE. Facing up to the global challenges of ageing. *Nature*. 2018 Sep;561(7721):45-56. doi: 10.1038/s41586-018-0457-8. Epub 2018 Sep 5. PMID: 30185958.
2. López-Otín C, Blasco MA, Partridge L, Serrano M, Kroemer G. The hallmarks of aging. *Cell*. 2013 Jun 6;153(6):1194-217. doi: 10.1016/j.cell.2013.05.039. PMID: 23746838; PMCID: PMC3836174.
3. Sarkisian CJ, Keister BA, Stairs DB, Boxer RB, Moody SE, Chodosh LA. Dose-dependent oncogene-induced senescence in vivo and its evasion during mammary tumorigenesis. *Nat Cell Biol*. 2007 May;9(5):493-505. doi: 10.1038/ncb1567. Epub 2007 Apr 22. PMID: 17450133.
4. Althubiti M, Lezina L, Carrera S, Jukes-Jones R, Giblett SM, Antonov A, Barlev N, Saldanha GS, Pritchard CA, Cain K, Macip S. Characterization of novel markers of senescence and their prognostic potential in cancer. *Cell Death Dis*. 2014 Nov 20;5(11):e1528. doi: 10.1038/cddis.2014.489. PMID: 25412306; PMCID: PMC4260747.
5. Serrano M, Lin AW, McCurrach ME, Beach D, Lowe SW. Oncogenic ras provokes premature cell senescence associated with accumulation of p53 and p16INK4a. *Cell*. 1997 Mar 7;88(5):593-602. doi: 10.1016/s0092-8674(00)81902-9. PMID: 9054499.

6. Collado M, Gil J, Efeyan A, Guerra C, Schuhmacher AJ, Barradas M, Benguría A, Zaballos A, Flores JM, Barbacid M, Beach D, Serrano M. Tumour biology: senescence in premalignant tumours. *Nature*. 2005 Aug 4;436(7051):642. doi: 10.1038/436642a. PMID: 16079833.
7. Chen Z, Trotman LC, Shaffer D, Lin HK, Dotan ZA, Niki M, Koutcher JA, Scher HI, Ludwig T, Gerald W, Cordon-Cardo C, Pandolfi PP. Crucial role of p53-dependent cellular senescence in suppression of Pten-deficient tumorigenesis. *Nature*. 2005 Aug 4;436(7051):725-30. doi: 10.1038/nature03918. PMID: 16079851; PMCID: PMC1939938.
8. Michaloglou C, Vredevelde LC, Soengas MS, Denoyelle C, Kuilman T, van der Horst CM, Majoer DM, Shay JW, Mooi WJ, Peeper DS. BRAFE600-associated senescence-like cell cycle arrest of human naevi. *Nature*. 2005 Aug 4;436(7051):720-4. doi: 10.1038/nature03890. PMID: 16079850.
9. Stupp R, Mason WP, van den Bent MJ, Weller M, Fisher B, Taphoorn MJ, Belanger K, Brandes AA, Marosi C, Bogdahn U, Curschmann J, Janzer RC, Ludwin SK, Gorlia T, Allgeier A, Lacombe D, Cairncross JG, Eisenhauer E, Mirimanoff RO, Radiotherapy plus concomitant and adjuvant temozolomide for glioblastoma. *The New England journal of medicine*. 2005 Mar 10. PMID: 15758009]
10. Kumari R, Jat P. Mechanisms of Cellular Senescence: Cell Cycle Arrest and Senescence Associated Secretory Phenotype. *Front Cell Dev Biol*. 2021 Mar 29; 9:645593. doi: 10.3389/fcell.2021.645593. PMID: 33855023; PMCID: PMC8039141.
11. Liggett WH Jr, Sidransky D. Role of the p16 tumor suppressor gene in cancer. *J Clin Oncol*. 1998 Mar;16(3):1197-206. doi: 10.1200/JCO.1998.16.3.1197. PMID: 9508208.
12. Rocco JW, Sidransky D. p16(MTS-1/CDKN2/INK4a) in cancer progression. *Exp Cell Res*. 2001 Mar 10;264(1):42-55. doi: 10.1006/excr.2000.5149. PMID: 11237522.
13. Gartel AL, Radhakrishnan SK. Lost in transcription: P21 repression, mechanisms, and consequences. *Cancer Res*. 2005 May 15;65(10):3980-5. doi: 10.1158/0008-5472.CAN-04-3995. PMID: 15899785.
14. Deng C, Zhang P, Harper JW, Elledge SJ, Leder P. Mice lacking P21CIP1/WAF1 undergo normal development, but are defective in G1 checkpoint control. *Cell*. 1995 Aug 25;82(4):675-84. doi: 10.1016/0092-8674(95)90039-x. PMID: 7664346.
15. Zilfou JT, Spector MS, Lowe SW. Slugging it out: fine tuning the p53-PUMA death connection. *Cell*. 2005 Nov 18;123(4):545-8. doi: 10.1016/j.cell.2005.11.003. PMID: 16286002; PMCID: PMC4578637.
16. Hall BM, Balan V, Gleiberman AS, Strom E, Krasnov P, Virtuoso LP, Rydkina E, Vujcic S, Balan K, Gitlin I, Leonova K, Polinsky A, Chernova OB, Gudkov AV. Aging of mice is associated with p16(Ink4a)- and β -galactosidase-positive macrophage accumulation that can be induced in young mice by senescent cells. *Aging (Albany NY)*. 2016 Jul;8(7):1294-315. doi: 10.18632/aging.100991. PMID: 27391570; PMCID: PMC4993332.
17. Hall BM, Balan V, Gleiberman AS, Strom E, Krasnov P, Virtuoso LP, Rydkina E, Vujcic S, Balan K, Gitlin II, Leonova KI, Consiglio CR, Gollnick SO, Chernova OB, Gudkov AV. p16(Ink4a) and senescence-associated β -galactosidase can be induced in macrophages as part of a reversible response to physiological stimuli. *Aging (Albany NY)*. 2017 Aug 2;9(8):1867-1884. doi: 10.18632/aging.101268. PMID: 28768895; PMCID: PMC5611982.
18. Rahman M, Olson I, Mansour M, Carlstrom LP, Sutiwisesak R, Saber R, Rajani K, Warrington AE, Howard A, Schroeder M, Chen S, Decker PA, Sananikone EF, Zhu Y, Tchkonja T, Parney IF, Burma S, Brown D, Rodriguez M, Sarkaria JN, Kirkland JL, Burns TC. Selective Vulnerability of Senescent Glioblastoma Cells to BCL-XL Inhibition. *Mol Cancer Res*. 2022 Jun 3;20(6):938-948. doi: 10.1158/1541-7786.MCR-21-0029. PMID: 35191501. Yeh AC, Ramaswamy S. Mechanisms of Cancer Cell Dormancy--Another Hallmark of Cancer? *Cancer Res*. 2015 Dec 1;75(23):5014-22. doi: 10.1158/0008-5472.CAN-15-1370. Epub 2015 Sep 9. PMID: 26354021; PMCID: PMC4668214.
19. Ahmed AU, Auffinger B, Lesniak MS. Understanding glioma stem cells: rationale, clinical relevance and therapeutic strategies. *Expert Rev Neurother*. 2013 May;13(5):545-55. doi: 10.1586/ern.13.42. PMID: 23621311; PMCID: PMC4524288.
20. Almog N. Molecular mechanisms underlying tumor dormancy. *Cancer Lett*. 2010 Aug 28;294(2):139-46. doi: 10.1016/j.canlet.2010.03.004. Epub 2010 Apr 2. PMID: 20363069.
21. Gulaia V, Kumeiko V, Shved N, Cicinskas E, Rybtsov S, Ruzov A, Kagansky A. Molecular Mechanisms Governing the Stem Cell's Fate in Brain Cancer: Factors of Stemness and Quiescence. *Front Cell Neurosci*. 2018 Nov 19; 12:388. doi: 10.3389/fncel.2018.00388. PMID: 30510501; PMCID: PMC6252330.
22. Triana-Martínez F, Loza MI, Domínguez E. Beyond Tumor Suppression: Senescence in Cancer Stemness and Tumor Dormancy. *Cells*. 2020 Feb 3;9(2):346. doi: 10.3390/cells9020346. PMID: 32028565; PMCID: PMC7072600.
23. Rossari F, Zucchinetti C, Buda G, Orciuolo E. Tumor dormancy as an alternative step in the development of chemoresistance and metastasis - clinical implications. *Cell Oncol (Dordr)*. 2020 Apr;43(2):155-176. doi: 10.1007/s13402-019-00467-7. Epub 2019 Aug 7. PMID: 31392521.
24. Spencer SL, Cappell SD, Tsai FC, Overton KW, Wang CL, Meyer T. The proliferation-quiescence decision is controlled by a bifurcation in CDK2 activity at mitotic exit. *Cell*. 2013 Oct 10;155(2):369-83. doi: 10.1016/j.cell.2013.08.062. Epub 2013 Sep 26. PMID: 24075009; PMCID: PMC4001917.
25. Stewart-Ornstein J, Lahav G. Dynamics of CDKN1A in Single Cells Defined by an Endogenous Fluorescent Tagging Toolkit. *Cell Rep*. 2016 Feb 23;14(7):1800-1811. doi: 10.1016/j.celrep.2016.01.045. Epub 2016 Feb 11. PMID: 26876176; PMCID: PMC5154611.
26. Kumar R, Paul AM, Amjesh R, George B, Pillai MR. Coordinated dysregulation of cancer progression by the HER family and P21-activated kinases. *Cancer Metastasis Rev*. 2020 Sep;39(3):583-601. doi: 10.1007/s10555-020-09922-6. Epub 2020 Aug 21. PMID: 32820388.

27. Klopffleisch R, Gruber AD. Differential expression of cell cycle regulators P21, p27 and p53 in metastasizing canine mammary adenocarcinomas versus normal mammary glands. *Res Vet Sci*. 2009 Aug;87(1):91-6. doi: 10.1016/j.rvsc.2008.12.010. Epub 2009 Jan 30. PMID: 19185891.
28. Klopffleisch R, von Euler H, Sarli G, Pinho SS, Gärtner F, Gruber AD. Molecular carcinogenesis of canine mammary tumors: news from an old disease. *Vet Pathol*. 2011 Jan;48(1):98-116. doi: 10.1177/0300985810390826. Epub 2010 Dec 13. PMID: 21149845.
29. Georgakilas AG, Martin OA, Bonner WM. P21: A Two-Faced Genome Guardian. *Trends Mol Med*. 2017 Apr;23(4):310-319. doi: 10.1016/j.molmed.2017.02.001. Epub 2017 Mar 7. PMID: 28279624.
30. Sikora E, Mosieniak G, Sliwinska MA. Morphological and Functional Characteristic of Senescent Cancer Cells. *Curr Drug Targets*. 2016;17(4):377-87. doi: 10.2174/1389450116666151019094724. PMID: 26477465.
31. Coppé JP, Patil CK, Rodier F, Sun Y, Muñoz DP, Goldstein J, Nelson PS, Desprez PY, Campisi J. Senescence-associated secretory phenotypes reveal cell-nonautonomous functions of oncogenic RAS and the p53 tumor suppressor. *PLoS Biol*. 2008 Dec 2;6(12):2853-68. doi: 10.1371/journal.pbio.0060301. PMID: 19053174; PMCID: PMC2592359.
32. Childs BG, Gluscevic M, Baker DJ, Laberge RM, Marquess D, Dananberg J, van Deursen JM. Senescent cells: an emerging target for diseases of ageing. *Nat Rev Drug Discov*. 2017 Oct;16(10):718-735. doi: 10.1038/nrd.2017.116. Epub 2017 Jul 21. PMID: 28729727; PMCID: PMC5942225.
33. Prata LGPL, Ovsyannikova IG, Tchkonina T, Kirkland JL. Senescent cell clearance by the immune system: Emerging therapeutic opportunities. *Semin Immunol*. 2018 Dec; 40:101275. doi: 10.1016/j.smim.2019.04.003. Epub 2019 May 11. PMID: 31088710; PMCID: PMC7061456.
34. Birch J, Gil J. Senescence and the SASP: many therapeutic avenues. *Genes Dev*. 2020 Dec 1;34(23-24):1565-1576. doi: 10.1101/gad.343129.120. PMID: 33262144; PMCID: PMC7706700.
35. Ito Y, Hoare M, Narita M. Spatial and Temporal Control of Senescence. *Trends Cell Biol*. 2017 Nov;27(11):820-832. doi: 10.1016/j.tcb.2017.07.004. Epub 2017 Aug 17. PMID: 28822679.
36. Nacarelli T, Lau L, Fukumoto T, Zundell J, Fatkhutdinov N, Wu S, Aird KM, Iwasaki O, Kossenkova AV, Schultz D, Noma KI, Baur JA, Schug Z, Tang HY, Speicher DW, David G, Zhang R. NAD⁺ metabolism governs the proinflammatory senescence-associated secretome. *Nat Cell Biol*. 2019 Mar;21(3):397-407. doi: 10.1038/s41556-019-0287-4. Epub 2019 Feb 18. PMID: 30778219; PMCID: PMC6448588.
37. Carlson BL, Pokorný JL, Schroeder MA, Sarkaria JN. Establishment, maintenance and in vitro and in vivo applications of primary human glioblastoma multiforme (GBM) xenograft models for translational biology studies and drug discovery. *Curr Protoc Pharmacol*. 2011 Mar; Chapter 14(14): Unit 14.16. doi: 10.1002/0471141755.ph1416s52. PMID: 21743824; PMCID: PMC3129784.